Available online at www.sciencedirect.com
ScienceDirect
Mathematics and Computers in Simulation 187 (2021) 155–170
MATHEMATICS AND COMPUTERS IN SIMULATION
www.elsevier.com/locate/matcom

Original Articles

Convective stability of a permeable nanofluid inside a horizontal conduit: Fast chemical reactions

Jawali C. Umavathi[a,*], Ali J. Chamkha[b,c]

[a] *Department of Mathematics, Gulbarga University, Gulbarga 585 106, Karnataka India*
[b] *Faculty of Engineering, Kuwait College of Science and Technology, Doha District, Kuwait*
[c] *Center of Excellence in Desalination Technology, King Abdulaziz University, P.O. Box 80200, Jeddah 21589, Saudi Arabia*

Received 20 October 2020; received in revised form 23 January 2021; accepted 16 February 2021
Available online 23 February 2021

Abstract

This problem considers the instabilities, which can occur when a horizontal sparsely filled nanofluid porous layer is saturated with a binary mixture with fast chemical reaction. The upper and lower plates are heated isothermally. The model used for the nanofluid incorporates the effects of Brownian motion and thermophoresis. The modified Darcy equation that includes the time derivative term is used to model the momentum equation. The energy equation includes cross and regular diffusion conditions. In conjunction with the Brownian motion, the nanoparticle fraction becomes stratified; hence the viscosity and the conductivity are stratified. The nanofluid is assumed to be diluted and this enables the porous medium to be treated as a weakly heterogeneous medium with variation, in the vertical direction, of conductivity and viscosity. The oscillatory and stationary convection are evaluated analytically. The reaction rate is supposed to be greater than the diffusion rate. We find that both a stationary instability and an oscillatory instability can occur as the first bifurcation, depending on the sign and the value of the heat of reaction. The execution of the porous parameter, Prandtl number, Soret parameter, Dufour parameter, Lewis number, solutal Rayleigh number, chemical reaction and the modified diffusivity ratio parameters is implemented pictorially. It is found that the presence of nanoparticles the critical Rayleigh number is increased and helps to stabilize the system. The presence of chemical reaction parameter destabilizes the system. The results of previously-published work are also obtained as special cases of the general solution.

Keywords: Nanofluid; Porous medium; Natural convection; Binary mixture; Chemical reaction; Brownian motion and thermophoresis

1. Introduction

Convective stability investigation for permeable fluids has been reviewed since about thirty years. Some of the application areas are solar energy conversion, underground coal gasification, extraction of geothermal energy. The applied gradients of temperature or concentration at the walls were the active forces at the time of the initial studies on stability. Employing a Rayleigh–Bernard type of convection, Lapwood [31], Davis [10], Beck [4] and Gershuni and Zhukhovitskii [14] assessed the onset of convection in the absence of chemical reactions. Recently, the focus is also on the study of convective instabilities in reactive fluids. In recent years there has been considerable

* Corresponding author.
E-mail addresses: drumavathi@rediffmail.com (J.C. Umavathi), a.chamkha@kcst.edu.kw (A.J. Chamkha).

https://doi.org/10.1016/j.matcom.2021.02.016

Nomenclature

A	Average specific heat
a	Dimensionless wave number
a_x, a_y	Wave numbers
C	Concentration
C_{eq}	Equilibrium state concentration
C_P	Specific heat
d	Thickness
F	Porous parameter, $\left(\frac{d^2}{k}\right)$
g	Gravity
K	Permeability
k_{eff}	Effective thermal conductivity
Le	Lewis number of thermo-solutal
Ln	Lewis number
N_A	Diffusivity ratio
N_B	Particle-density increment
N_{CT}	Soret number
N_{TC}	Dufour number
Pr	Prandtl number, $\left(\frac{\nu}{\kappa}\right)$
p	Pressure
R	Rayleigh number, $\left(\frac{g\alpha T_z d^4}{\kappa\nu}\right)$
Rm	Basic-density Rayleigh number
Rn	Solutal Rayleigh number
T	Temperature
T_z	Temperature gradient
t	Time
t_r	Chemical reaction relaxation time
X	Dimensionless parameter,
$(x,\ y,\ z)$	Co-ordinates

Greek symbols

α_C	Coefficient of solute expansion
α_T	Coefficient thermal expansion
ε	Porosity
κ	Diffusivity
μ	Viscosity
μ_e	Brinkman viscosity
μ_{eff}	Effective viscosity
λ	Heat conductivity
ν	Kinematic viscosity
ρ	Density
ϕ	Reaction of heat
σ	Growth rate
η	Non-dimensional parameter, $\left(\frac{\phi\tau_2}{\tau_1}\right)$
ψ	Reaction parameter, $\left(\frac{\phi\alpha_C}{\alpha_T}\right)$

ω	Frequency
φ	Relative nanoparticle volume fraction, $\frac{\phi^*-\phi_0^*}{\phi_1^*-\phi_0^*}$
Superscripts	
*	Non-dimensional quantity
$'$	Perturbed quantity
Subscripts	
0	Reference value
f	Fluid
s	Solid
r	Reference

interest, from various branches of fluid mechanics and condensed matter physics, in systems that show an oscillatory instability as the first bifurcation. On the other hand, use of a porous medium significantly simplifies the descriptions of an average hydrodynamic flow and allows us to consider realistic boundary conditions for the velocity. Therefore, the considered system is expected to be a convenient object for studying the nonlinear behavior above the critical level.

The Russian school (Zeldovich and Frank-Kamenetskii [64], Frank-Kamenetskii [13]) designed the solid–fluid system in the presence of chemical reaction. Varma and Aris [59], contributed a diagram of the bifurcation which possessed a maximum of three solutions. Viljoen et al. [60] suggested that an adiabatic reacting system always will have the maximum of three solutions. The effect of fast chemical reaction on the stability of a binary mixtures with porous medium was studied by Stainberg and Brand [45]. They pointed out that either monotonic or oscillatory instabilities can flourish at the first bifurcation point. Viljoen and Hlavacek [61] presented convective instabilities for a zero-order reaction. Rudraiah et al. [44] and Rudraiah and Malashetty [43] resolved the stability for the binary mixture of the permeable fluid. The stability convection with or without reactions was examined by Malashetty and Gaikwad [32]. They remarked that the effect of increasing the chemical reaction parameter was to decrease the critical Rayleigh number for both stationary and oscillatory states and hence the presence of chemical reaction parameter was to destabilize the system.

More energy efficiency is not possible if the conductivity of the heat is small. By suspending particles of a nano-size in working fluids such as water, oil, ethylene-glycol, etc., a nanofluid is prepared. Several researchers (Eastman et al. [12], Bianco et al. [6], Khanafer and Vafai [30]) have proved that the thermal conductivity can be hiked by more than 20% by suspending nanoparticles. Three-dimensional rotating flow of water-based carbon nanotubes was investigated by Hayat et al. [16] in the presence of Darcy–Forchheimer porous space and homogeneous–heterogeneous reactions. Their findings indicated that the skin friction coefficients and local Nusselt number were enhanced for larger values of nanoparticles volume fraction. Aziz et al. [3] discussed the 3D rotating flow of nanoliquid in the presence of Darcy–Forchheimer porous space and homogeneous–heterogeneous reactions. They revealed that an enhancement in thermophoresis parameter yields stronger thermal and concentration fields while opposite behavior was observed for higher Brownian motion parameter. They also noticed that impacts of porosity parameter and Forchheimer number on the thermal and concentration fields were quite similar while reverse trend was seen for concentration rate. Hayat et al. [15] numerically computed the Darcy–Forchheimer flow of nanofluid due to a rotating disk with convective heat and mass conditions. They found that the larger concentration Biot number exhibits increasing behavior for both concentration and its associated layer thickness. Numerical simulation for Darcy–Forchheimer 3D rotating flow subject to binary chemical reaction and Arrhenius activation energy was investigation by Hayat et al. [17]. They concluded that the Brownian motion parameter for temperature and concentration has reverse effects while similar trend was observed via thermophoresis parameter.

The free convection flow of nanoparticles such as Al_2O_3 and CuO suspended in a water base in a cylinder was explored by Putra et al. [42]. They reported that increasing the number of the nanoparticles suppresses the rate of energy. Analysis of entropy generation for MHD flow of third grade nanofluid over a nonlinear stretching surface embedded in a porous medium was researched by Hayat et al. [21]. They found that the activation energy

reduced the concentration boundary layer thickness. The entropy was promoted with temperature difference variable, Brinkman number, porosity parameter, radiation parameter and magnetic parameter. Hayat et al. [22] also addressed the influence of binary chemical reaction and activation energy in hydromagnetic flow of third grade nanofluid using convective conditions. They observed that the temperature and concentration distribution were enhanced for large values of thermal and concentration Biot numbers. The MHD three-dimensional flow of viscous nanofluid adopting convective conditions was explored by Hayat et al. [18]. Hayat et al. [19] also addressed the flow of Carreau liquid in the presence of nanomaterials induced by nonlinearly extendable surface. They claimed that for all values of flow behavior index, Brownian movement number enhanced the temperature whereas it reduced the concentration fields.

In nanofluid flows, there are many mechanisms namely; thermophoresis and Brownian motion (Probstein [41]). The seven mechanisms between fluid and nanoparticles were introduced by Buongiorno [8]. The Dufour, Brownian motion and thermophoresis were ramified by Pakravan and Yaghoubi [40]. Umavathi and her group (Umavathi et al. [51], Umavathi and Sheremet [57], Marudappa and Umavathi [33], Umavathi et al. [55], Diglio et al. [11]) examined the nanofluid properties in various geometries.

Impact of Cattaneo–Christov heat flux model in flow of variable thermal conductivity fluid over a variable thicked surface was studied by Hayat et al. [20]. They concluded that both thermally stratified and solutal stratified parameters decay the temperature and concentration. Colloidal study of Casson fluid with homogeneous–heterogeneous reactions was carried out by Khan et al. [26] and they found that the drag force was enhanced for large Hartman number and for large Prandtl number the rate of heat transfer was reduced. Khan et al. [28] also investigated the simulation and modeling of second order velocity slip flow of micropolar ferrofluid with Darcy–Forchheimer porous medium. Flow and thermal analysis on Darcy–Forchheimer flow of copper–water nanofluid due to a rotating disk were researched by Nayak et al. [38]. They claimed that the porous matrix reduced the velocity but elevated the temperature distribution and the entropy was minimized with large values of Brinkman and Reynolds number. Entropy analysis using Darcy–Forchheimer nanofluid for variable temperature was also discussed by Abbas et al. [2] and they found that entropy generation and Bejan number were contracted for higher values of Brinkman number. Abbas et al. [1] investigated the entropy optimized second order velocity slip MHD nanofluid flow activation energy.

Khan et al. [24] researched the mixed convective nanoliquid slip flow of Walter-B fluid subject to stretched surface with gyrotactic microorganisms. They concluded that the concentration field decays with higher values of Schmidt number and enhanced by increasing the values of activation energy parameter. Wang et al. [63] investigated the irreversible aspects in mangetohydrodynamics flow of viscous nanofluid by a variable thicked surface. Wang et al. [62] also worked on the transportation of heat generation/absorption and radiative heat flux in homogeneous–heterogeneous catalytic reactions using Oldroyd-B model. Muhammad et al. [35] worked on the MHD radiated nanomaterial viscous material flow by a curved surface with second order slip and entropy generation. They marked that the velocity was demoted with first order slip parameter and heterogeneous reaction parameter upsurged the Bejan number and entropy generation. The numerical computations were carried out by Khan and Alzahrani [25] on the activation energy and binary chemical reaction effect in nonlinear thermal radiative stagnation point flow of Walter-B nanofluid. They identified that the higher values of thermal Biot number enhanced the temperature. Fully developed Darcy–Forchheimer mixed convective flow over a curved surface with activation energy and entropy generation was surveyed by Muhammad et al. [36]. They found that the entropy generation was enhanced with diffusion parameter and chemical reaction parameter. Khan et al. [29] worked out on the modeling of Cattaneo–Christov double diffusions (CCDD) in Williamson nanomaterial slip flow subject to porous medium. They marked that the skin friction coefficient was reduced for higher values of Weissenberg number and slip parameter. Mathematical modeling and analysis of SWCNT–Water and MWCNT–Water flow over a stretchable sheet were investigated by Ibrahim and Khan [23]. Velocity was dominant in SWCNT–Water over MWCNT–Water whereas temperature was dominant in MWCNT–Water over SWCNT–Water. Nayak et al. [37] researched on the three dimensional unsteady magnetohydrodynamic flow and entropy generation of micropolar Casson Cross nanofluid subject to nonlinear thermal radiation and chemical reaction. They showed that strengthening of Weissenberg number uplifts the axial as well as transverse fluid velocities while that of Hartmann number turns out to be showing a reverse trend. Irreversibility analysis and heat transport in squeezing nanoliquid flow of non-Newtonian (Second Grade) fluid between infinite plates with activation energy were studied by Khan et al. [27]. The squeezing parameter causes the velocity to enhance and reduce the temperature.

Nield and Kuznestov [39] researched the stability inside a channel packed with a permeable nanofluid. They found that oscillatory convection developed for the bottom-heavy nanoparticle distribution. Following the work of

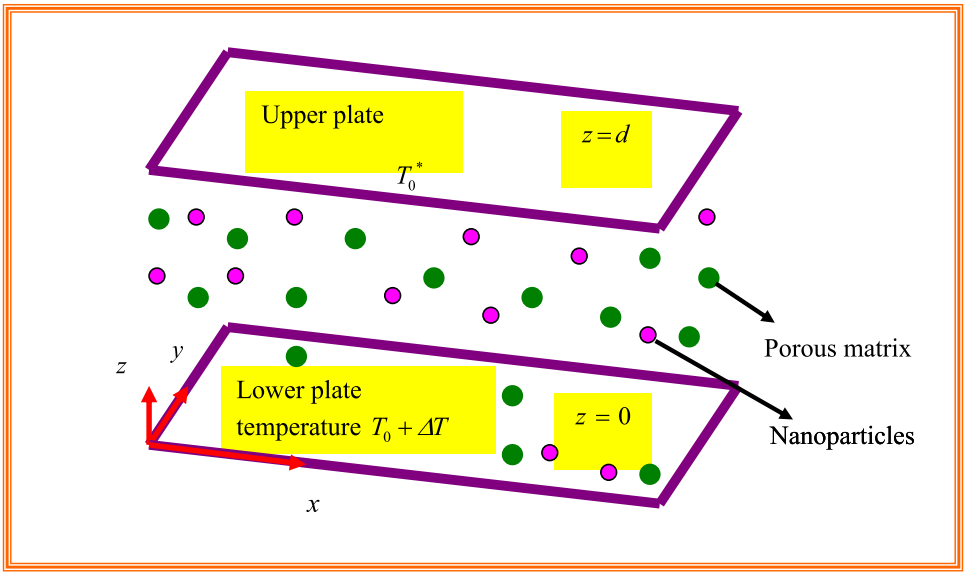

Fig. 1. Geometric model of a nanofluid layer in a rigid porous medium microfluidic channel.

Nield and Kuznestov [39], Umavathi and her group (Umavathi [47–49], Umavathi and Mohite [52–54], Umavathi et al. [50], Umavathi and Prathap Kumar [56], Umavathi and Sheremet [58]) measured the thermal instabilities and thermal modulation of Newtonian/non-Newtonian fluids saturated with a porous matrix and a nanofluid. The permeable nanofluid planted in a horizontal channel was probed by Chand and Rana [9] and Bhadauria et al. [5]. The conclusions admit that the thermal instability becomes stationary upon increasing the horizontal wave number.

The purpose of this paper is to research the linear stability analysis of the chemically driven instability of a reactive binary mixture in a sparsely packed porous medium saturated with nanofluid as this study is not carried out so far. To scrutinize the enforcement of the reaction due to the addition of mixtures, two approximations are implemented. First, we do not consider the influence of thermal diffusions for the reason that its presence on the stability is much smaller in comparison with the chemical reaction. Thus, we consider only the instability caused due to the chemical reactions. Secondly, we presume that the rate of diffusion is slow when compared with the external temperature gradient. In this resemblance, the stability investigation is simplified and hence, the analytic analysis for a realistic boundary conditions is possible. The motivation to take study on this topic is due to its applications in tubular reactors, oxidation of solid materials and synthesis of ceramic materials.

2. Mathematical formulation

The physical structure consists of a nanofluid binary reactive mixture immersed in a porous bed enfolded between parallel plates having a depth d and extended infinitely in the (x, y) plane as shown in Fig. 1. The gravity and temperature gradients are perpendicular to the plates. Each boundary wall is assumed to be perfectly thermally conducting. The temperatures at the lower and upper boundary are taken as $T_0 + \Delta T$ and T. The Oberbeck–Boussinesq approximation is employed. In the linear stability theory being applied here, the temperature change in the fluid is assumed to be small in comparison with T_0. The balance laws were accorded by Nield and Kuznestov [20] (for the stability equations) and Malashetty and Gaikwad [30] (for the fast chemical reaction).

The conservation equation takes the form

$$\nabla . q = 0 \tag{1}$$

Here q is the nanofluid Darcy velocity.

In the presence of thermophoresis, the conservation equation for the nanoparticles takes the form

$$\frac{\partial \phi}{\partial t} + \varepsilon^{-1} q . \nabla \phi = \nabla . \left[D_B \nabla \phi + D_T \frac{\nabla T}{T} \right] \tag{2}$$

where ϕ is the nanoparticle specific heat of the material constituting the nanoparticles, ε is the porosity, T is the temperature, D_B is the Brownian diffusion coefficient, and D_T is the thermophoretic diffusion coefficient.

If one introduces a buoyancy force and adopts the Boussinesq approximation, and uses the Darcy model for a porous medium, then the momentum equation can be written as

$$\frac{\partial q}{\partial t} + q.\nabla q = -\frac{\nabla p}{\rho_0} + \frac{\rho}{\rho_0}\mathrm{g} - \frac{\mu_{eff}}{\rho_0 K}q + \frac{\mu_e}{\rho_0}\nabla^2 q \tag{3}$$

Here K is the permeability of the porous medium, μ is the fluid viscosity and μ_e is the effective viscosity and ρ is the overall density of the nanofluid, which we now assume to be given by

$$\rho = \phi\rho_{\mathrm{p}} + (1-\phi)\,\rho_0\,[1-\alpha_T\,(T-T_0) + \alpha_C\,(C-C_0)] \tag{4}$$

where ρ_p is the particle density, ρ_0 is the reference density for the fluid, α_T and α_C are the thermal and solute expansion coefficients. The thermal energy equation for a nanofluid in the presence of fast chemical reactions can be written as

$$A\frac{\partial T}{\partial t} + q.\nabla T = k\nabla^2 T + \frac{C-C_{eq}}{\tau_1} + \frac{\varepsilon\,(\rho c)_{\mathrm{p}}}{(\rho c)_{\mathrm{f}}}\left[D_{\mathrm{B}}\nabla\phi.\nabla T + D_{\mathrm{T}}\frac{\nabla T.\nabla T}{T_0}\right] + \frac{(\rho c)_{\mathrm{p}}}{(\rho c)_{\mathrm{f}}}D_{TC}\nabla^2 C \tag{5}$$

Here c is the fluid specific heat (at constant pressure), c_p is the nanoparticle specific heat of the material constituting the nanoparticles, D_{TC} is a diffusivity of Dufour type, C_{eq} is the concentration in equilibrium state, k is the renormalized thermal diffusivity containing contribution from the porous medium and the nanofluid $A = \rho C_P/(\rho C_P)_f$, $\kappa = \lambda/(\rho C_P)$ where $\rho C_P = (1-\varepsilon)(\rho C_P)_s + \varepsilon(\rho C_P)_f$ and $\lambda = (1-\varepsilon)\lambda_s + \varepsilon\lambda_f$ are the average specific heat and heat conductivity respectively; the indices s and f correspond to particle and fluid respectively. $\tau_1 = t_r\rho C_P\left[T\left(\frac{\partial p_C}{\partial T}\right)_{P,C}\right]^{-1}$ t_r is the relaxation time of the chemical reaction, C_p is the specific heat at constant pressure, p_c is the chemical potential.

To this we add a conservation equation for the solute of the form

$$\frac{\partial C}{\partial t} + q.\nabla T = D_{sm}\nabla^2 C + D_{CT}\nabla^2 T - \frac{C-C_{eq}}{\tau_2} \tag{6}$$

where D_{sm} is the solute diffusivity for the porous medium and D_{CT} is a diffusivity of Soret type. It has been assumed that the nanoparticles do not affect the transport of the solute and $\tau_2 = t_r\rho$.

Further $k = \varepsilon k_{eff} + (1-\varepsilon)k_s$ where k_{eff} is the effective conductivity of the nanofluid (fluid plus nanoparticles), and k_s is the conductivity of the solid material forming the matrix of the porous medium. We now introduce the viscosity and the conductivity dependence on nanoparticle fraction. Following Tiwari and Das [46], we adopt the formulas, based on a theory of mixtures,

$\frac{\mu_{eff}}{\mu_f} = \frac{1}{(1-\phi)^{2.5}}$ is as defined in Brinkman [7] and $\frac{k_{eff}}{k_f} = \frac{(k_p+2k_f)-2\phi(k_f-k_p)}{(k_p+2k_f)+\phi(k_f-k_p)}$ is following Maxwell [34]. Here k_f and k_p are the thermal conductivities of the fluid and the nanoparticles, respectively. In the case where ϕ is small compared with unity, we can approximate these formulas by $\frac{\mu_{eff}}{\mu_f} = 1 + 2.5\phi^*$, $\frac{k_{eff}}{k_f} = \frac{(k_p+2k_f)-2\phi^*(k_f-k_p)}{(k_p+2k_f)+\phi^*(k_f-k_p)} = 1 + 3\phi^*\frac{(k_p-k_f)}{(k_p+2k_f)}$.

It is guessed that the Brinkman viscosity and the fluid viscosity are equal.($\mu_e = \mu$). It is also inferred that the diffusion rate is slow in connection with the reaction occurring due to the chemicals. The value of A is considered to be 1. It is well known that in the convection free steady state, in contrast to nonreactive fluids, the temperature and concentration gradients depend in the general case of reactive fluids on the vertical coordinate z. This makes the stability analysis considerably more difficult for an analytical approach. However, in the case of a fast chemical reaction considered here, Eqs. (1)–(6) admit the following stationary solution.

$$q = 0, \nabla T_0 = -T_z\hat{g}, \nabla\phi_0 = -\phi_z\hat{g}, \quad C = C_{eq}(T) \tag{7}$$

where T_z denotes the applied temperature gradient and it takes both positive and negative values and $\hat{g} = \vec{g}/\left|\vec{g}\right|$. At the lower boundary, the value of concentration C_0 and temperature T_0 in the form of power series expansion for $C_{eq} = C_{eq}(T)$ is taken as

$$C_{eq} = C_0 + \phi(T - T_0) \tag{8}$$

where ϕ is the heat of reaction parameter. Eq. (8) now takes the form as

$$\nabla C_0 = \phi \nabla T_0 \tag{9}$$

There are two types of settings on the boundary to define the concentration. For analytical computations, it is appropriate to have concentrations to be in equilibrium on the boundaries. Impermeable boundaries (zero mass flux) are incorporated and also it is assumed that on the boundaries, the concentrations are constant. The settings on the boundary for the momentum are taken as rigid–rigid or free–free or rigid–free. In all the cases, the consequence remains the same, although the Rayleigh numbers at the critical point are distinct. Thus, free boundaries are taken into account for the analysis.

The nonlinear equations become

$$\frac{\partial q}{\partial t} + q.\nabla q = -\frac{\nabla p}{\rho_0} + \left(\alpha_T T' + \alpha_C C'\right)\hat{\mathrm{g}} - \phi\left(\alpha_T T' + \alpha_C C'\right)\hat{\mathrm{g}} + \left(\phi - 1 - \phi\frac{\rho_P}{\rho_0}\right)\hat{\mathrm{g}} - \frac{\nu}{k}q + \nu\,\nabla^2 q \tag{10}$$

$$\frac{\partial T'}{\partial t} + q.\nabla T' - T_z\left(q.\hat{g}\right) = k\nabla^2 T' + \frac{C - C_{eq}}{\tau_1} + \frac{\varepsilon\,(\rho c)_{\mathrm{p}}}{(\rho c)_{\mathrm{f}}}\left[D_{\mathrm{B}}\nabla\phi.\nabla T' + D_{\mathrm{T}}\frac{\nabla T'.\nabla T'}{T_0}\right] + \frac{(\rho c)}{(\rho c)_{\mathrm{f}}}D_{TC}\nabla^2 C' \tag{11}$$

$$\frac{\partial C'}{\partial t} + q.\nabla T' - \phi T_z\left(q.\hat{g}\right) = D_{sm}\nabla^2 C' + D_{CT}\nabla^2 T' - \frac{C - C_{eq}}{\tau_2} \tag{12}$$

$$\frac{\partial \phi'}{\partial t} + \varepsilon^{-1} q.\nabla\phi = D_B\nabla^2\phi' + \frac{D_T}{T_C}\nabla^2 T' \tag{13}$$

Following the discussions as mentioned above on the status at the boundary yields the following:

$$w = \frac{\partial^2 w}{\partial z^2} = 0,\ T' = \phi' = C' = 0 at z = 0, d \tag{14}$$

Here, a prime denotes unsteady state solutions.

2.1. Linear stability analysis

After linearizing Eqs. (10)–(13) the reduced equations are

$$\frac{\partial q'}{\partial t} = -\frac{\nabla p}{\rho_0} + \left(\alpha_T T' + \alpha_C C'\right)\hat{\mathrm{g}} - \phi\left(\alpha_T T' + \alpha_C C'\right)\hat{\mathrm{g}} + \left(\phi - 1 - \phi\frac{\rho_P}{\rho_0}\right)\hat{\mathrm{g}} - \frac{\nu}{k}q' + \nu\,\nabla^2 q' \tag{15}$$

$$\frac{\partial T'}{\partial t} - T_z\left(q'.\hat{g}\right) = k\nabla^2 T' + \frac{C - C_{eq}}{\tau_1} + \frac{\varepsilon\,(\rho c)_{\mathrm{p}}}{(\rho c)_{\mathrm{f}}}\left[D_{\mathrm{B}}\nabla\phi.\nabla T' + D_{\mathrm{T}}\frac{\nabla T'.\nabla T'}{T_0}\right] + \frac{(\rho c)}{(\rho c)_{\mathrm{f}}}D_{TC}\nabla^2 C' \tag{16}$$

$$\frac{\partial C'}{\partial t} - \phi T_z\left(q.\hat{g}\right) = D_{sm}\nabla^2 C' + D_{CT}\nabla^2 T' - \frac{C - C_{eq}}{\tau_2} \tag{17}$$

$$\frac{\partial \phi'}{\partial t} = D_B\nabla^2\phi' + \frac{D_T}{T_C}\nabla^2 T' \tag{18}$$

After eliminating p' from Eq. (15), the resulting equations are made dimensionless by the following relations:

$$w^* = \frac{d}{\kappa}w',\ t^* = \frac{\kappa}{d^2}t,\ (x^*, y^*, z^*) = \frac{1}{d}(x, y, z),\ T^* = \frac{T'}{|\nabla T_0|\,d},\ C^* = \frac{C'}{|\nabla C_0|\,d},\ \phi = \frac{\phi^* - \phi_0^*}{\phi_1^* - \phi_0^*},\ \mathrm{Pr} = \frac{\nu}{\kappa}$$

$$F = \frac{d^2}{k},\ R = \frac{g\alpha T_z d^4}{\kappa\nu},\ Ln = \frac{\kappa}{D_B},\ Le = \frac{\kappa}{D_{Sm}},\ N_{CT} = \frac{D_{CT}}{\kappa},\ N_{TC} = \frac{(\rho C)\,\phi D_T}{(\rho C)_f\,\kappa},\ N_A = \frac{D_T\,|\nabla T_0|\,d}{D_B T_C\,(\phi_1 - \phi_0)}$$

$$N_B = \frac{\varepsilon\,(\rho C)_p\,(\phi_1 - \phi_0)}{(\rho C)_f},\ Rn = \left[\left(\frac{\rho_P}{\rho_0} - 1\right)(\phi_1 - \phi_0)\right]\frac{d^3\phi}{\kappa\nu},\ Rm = \left[\frac{\rho_P}{\rho_0}\phi + (1 - \phi_0)\right]\frac{d^3}{\kappa\nu} \tag{19}$$

The dimensionless equations then take the following form (dropping asterisks)

$$\left(\mathrm{Pr}^{-1}\frac{\partial}{\partial t} + F - \nabla^2\right)\nabla^2 w = R\left[\nabla_1^2 T' + \phi\frac{\alpha_C}{\alpha_T}\nabla_1^2 C'\right] - Rn\,\nabla_1^2\phi' \tag{20}$$

$$\left(\frac{\partial}{\partial t}-\nabla^2+\frac{\phi d^2}{\kappa\tau_1}\right)T=w+\left(\frac{\phi d^2}{\kappa\tau_1}\right)C+N_{TC}\nabla^2 C \tag{21}$$

$$\left(\frac{\partial}{\partial t}+\frac{d^2}{\kappa\tau_2}+\frac{1}{Le}\nabla^2\right)C=w+\left(\frac{d^2}{\kappa\tau_2}\right)T+N_{CT}\nabla^2 T \tag{22}$$

$$\frac{\partial\phi}{\partial t}+\frac{1}{\varepsilon}w=\frac{1}{Ln}\nabla^2\phi+\frac{N_A}{Ln}\nabla^2 T \tag{23}$$

where Rm is not included in the consecutive scrutiny as it is the static state pressure gradient.

3. Method of solution

We now assess the solutions as follows:

$$\begin{bmatrix} w(x,y,z,t)\\ T(x,y,z,t)\\ C(x,y,z,t)\\ \varphi(x,y,z,t)\end{bmatrix}=\begin{bmatrix} W\\ T\\ C\\ \varphi\end{bmatrix}e^{st}\sin\pi z\cos a_x x\cos a_y y \tag{24}$$

Substituting (24) into (20)–(23) we get the following equations:

$$\left(\overset{-1}{\Pr}s+F+\pi^2+a^2\right)\left(\pi^2+a^2\right)W=Ra^2\left[T+\psi\,C\right]-Rn\,a^2\varphi \tag{25}$$

$$\left(s+\pi^2+a^2+\frac{\phi d^2}{\kappa\tau_1}\right)T=W+\left(\frac{\phi d^2}{\kappa\tau_1}\right)C+N_{TC}\left(\pi^2+a^2\right)C \tag{26}$$

$$\left(s+\frac{d^2}{\kappa\tau_2}+\frac{\pi^2+a^2}{Le}\right)C=W+\left(\frac{d^2}{\kappa\tau_2}\right)T+N_{CT}\left(\pi^2+a^2\right)T \tag{27}$$

$$\frac{1}{\varepsilon}W-\frac{N_A}{Ln}\left(\pi^2+\alpha^2\right)T-\left(\frac{\left(\pi^2+\alpha^2\right)}{Ln}+s\right)\varphi=0 \tag{28}$$

where $a^2={a_x}^2+{a_y}^2$ and $\psi=\phi\frac{\alpha_C}{\alpha_T}$. Eliminating $W,\ T,\ C,\varphi$ from Eqs. (25)–(28), the relation for the thermal Rayleigh number, R is obtained as

$$R=\frac{1}{a^2\left(\frac{\pi^2+a^2}{Ln}+s\right)}\left[\begin{array}{l} N_{CT}\left(\pi^2+a^2\right)-s-X-\dfrac{\left(\pi^2+a^2\right)}{Le}-X\eta+N_{TC}\left(\pi^2+a^2\right)-\\ \psi\left(X+s+\pi^2+a^2+X\eta\right)\end{array}\right]^{-1}$$
$$\left[\begin{array}{l}\left(s\,\mathrm{Pr}^{-1}+F+\pi^2+a^2\right)\left(\pi^2+a^2\right)\left(s+\pi^2+a^2+X\eta\right)\left(\dfrac{\pi^2+a^2}{Ln}+s\right)\\ \left(N_{CT}\left(\pi^2+a^2\right)-s-X-\dfrac{\left(\pi^2+a^2\right)}{Le}\right)+\left(X\eta+N_{TC}\left(\pi^2+a^2\right)\right)X\left(\dfrac{\pi^2+a^2}{Ln}+s\right)\\ -\left(Rna^2\right)\frac{N_A}{Ln}\left(\pi^2+a^2\right)\left(N_{CT}\left(\pi^2+a^2\right)-s-X-\dfrac{\left(\pi^2+a^2\right)}{Le}\right)+\\ \dfrac{1}{\varepsilon}\left(s+\pi^2+a^2+X\eta\right)\left(s+X+\dfrac{\pi^2+a^2}{Le}-N_{CT}\left(\pi^2+a^2\right)\right)\\ -\left(X\eta+N_{TC}\left(\pi^2+a^2\right)\right)\left(\dfrac{N_A}{Ln}\left(\pi^2+a^2\right)+\dfrac{X}{\varepsilon}\right)\end{array}\right] \tag{29}$$

Here $X=\frac{d^2}{\kappa\tau_2}$, $\eta=\frac{\phi\tau_2}{\tau_1}$ and the linear stability is discussed for two modes, viz., stationary mode and the oscillatory modes.

3.1. Stationary mode

At the marginal state, $s\ (=s_r+i\,s_i=0, s_r=s_i=0)=0$. The steady-state Rayleigh number is as follows:

$$R=\frac{1}{a^2\left(\frac{\pi^2+a^2}{Ln}\right)}\left[\begin{array}{l} N_{CT}\left(\pi^2+a^2\right)-X-\dfrac{\left(\pi^2+a^2\right)}{Le}-X\eta+N_{TC}\left(\pi^2+a^2\right)- \\ \psi\left(X+\pi^2+a^2+X\eta\right)\end{array}\right]^{-1}$$
$$\left[\begin{array}{l}\left(F+\pi^2+a^2\right)\left(\pi^2+a^2\right)\left(\pi^2+a^2+X\eta\right)\left(\dfrac{\pi^2+a^2}{Ln}\right) \\ \left(N_{CT}\left(\pi^2+a^2\right)-X-\dfrac{\left(\pi^2+a^2\right)}{Le}\right)+\left(X\eta+N_{TC}\left(\pi^2+a^2\right)\right)X\left(\dfrac{\pi^2+a^2}{Ln}\right) \\ -\left(Rna^2\right)\frac{N_A}{Ln}\left(\pi^2+a^2\right)\left(N_{CT}\left(\pi^2+a^2\right)-X-\dfrac{\left(\pi^2+a^2\right)}{Le}\right)+ \\ \dfrac{1}{\varepsilon}\left(\pi^2+a^2+X\eta\right)\left(X+\dfrac{\pi^2+a^2}{Le}-N_{CT}\left(\pi^2+a^2\right)\right) \\ -\left(X\eta+N_{TC}\left(\pi^2+a^2\right)\right)\left(\dfrac{N_A}{Ln}\left(\pi^2+a^2\right)+\dfrac{X}{\varepsilon}\right)\end{array}\right] \tag{30}$$

Minimizing the above definition for the term a^2 and evaluating the reduced equation for a^2 give the critical wave number a_c. The critical Rayleigh number R_c for the stationary instability is calculated by substituting a_c into Eq. (30).

3.2. Oscillatory mode

Considering $s=i\omega$, where ω is real and positive. For the oscillatory mode the Rayleigh number is obtained by the process of conjugation as follows

$$R=\Delta_1+i\,\omega\,\Delta_2 \tag{31}$$

For an oscillatory onset $\Delta_2=0\,(\omega\neq 0)$ which results in obtaining the relation for the dispersion (on draining the subscript i)

$$b_1\left(\omega^2\right)^2+b_2\left(\omega^2\right)+b_3=0 \tag{32}$$

Now. Eq. (31) with $\Delta_2=0$ reduces to

$$R=a_0\left(a_1+\omega^2 a_2\right) \tag{33}$$

Δ_1, Δ_2, b_i and a_i $(i=1,2,3)$ are not conferred for brevity.

4. Results and discussion

In the present study we have employed a linear stability analysis for chemically driven instabilities in a binary mixture with a chemical reaction that is fast compared with the diffusion rate. Analytical expressions have found for the onset of stationary, oscillatory instabilities and oscillatory frequency, which depend on the rate and the heat of reaction. The critical wave number also depends strongly on these quantities.

Fig. 2(a–i) represent the graphs of stationary convection. In these graphs, the effects of various values of 'a' and Ra (Rayleigh number) for fixed values of F, Pr, η, N_{CT}, N_{TC}, Rn, Ln, N_A, and ψ for the stationary case are presented. Fig. 2a depicts the stability curves for diverse values of porous parameter$F$. It is seen from this figure that an increase in the value of the porous parameter increases the critical Rayleigh number of the stationary mode. Physically this implies that the presence of porous matrix stabilizes the system Fig. 2b illustrates the deviation of Ra with a for distinct values of Pr. This graph appraises that the Prandtl number does not impress the stationary convection. That it is to say that Prandtl number does not disturb the system significantly. Fig. 2c characterizes the impact of η, and as η increases Ra is reduced which indicates that the parameter η destabilizes the system (similar result was obtained by Malashetty and Gaikwad [32]). From Fig. 2 d, e, f, we observe that the enforcement of N_{CT},

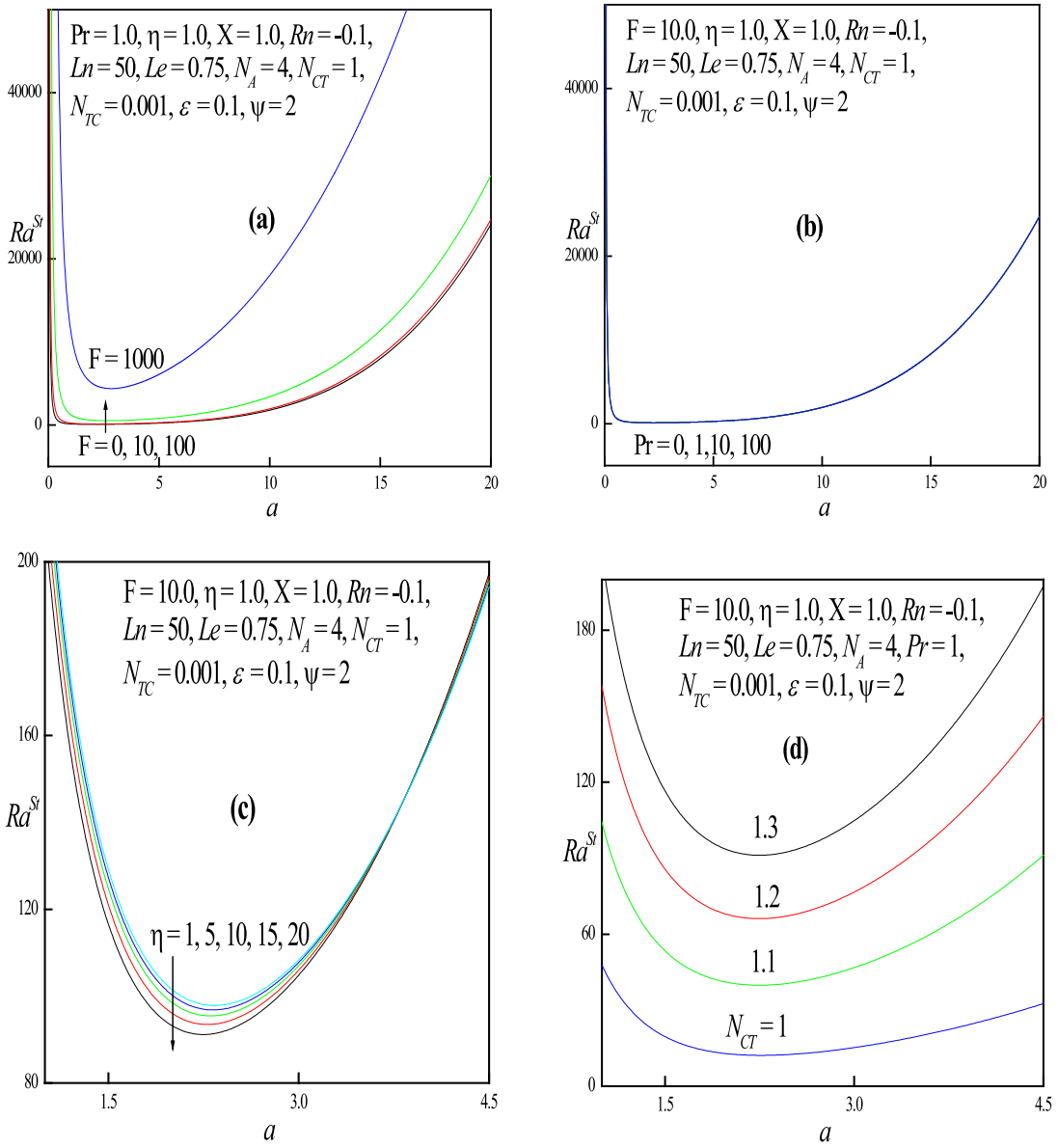

Fig. 2. Ra versus a for various **(a)** F **(b)** Pr **(c)** η **(d)** N_{CT} **(e)** N_{TC} **(f)** Rn **(g)** Ln **(h)** N_A and **(i)** ψ for the stationary case.

N_{TC}, and Rn is to increase Ra and hence they help to stabilize the system. (similar result as obtained by Bhadauria and Agarwal [5]). From Fig. 2g, we mark that the Rayleigh number is advanced by boosting the Lewis number Ln, which infers that Ln stabilizes the convection and hence, strengthens the marginal stability. Fig. 2h indicates that as N_A increases (for both positive and negative values) that the Rayleigh number is reduced and hence it destabilizes the system (similar result observed by Chand and Rana [9]). Effect of increasing the chemical reaction parameter ψ is to decrease the Rayleigh number and hence it destabilizes the system (similar result obtained by Malashetty and Gaikwad [32]).

Fig. 3(a–h) are the profiles for the specific values of Ra and a for individual values of the governing parameters F, Pr, N_{CT}, N_{TC}, Rn, Ln, N_A, and ψ for the oscillatory case. Figs. 3a and 3b depict the effect of porous parameter F and Prandtl number Pr on the Rayleigh number respectively. The Rayleigh number increases with increase in both F and Pr which suggest that these parameters help to stabilize the system which was the similar result observed by

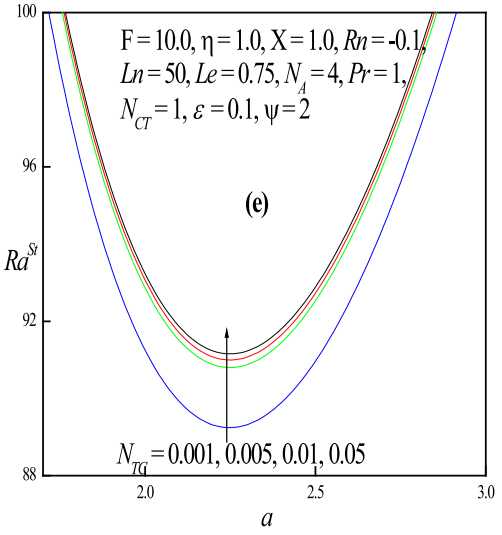

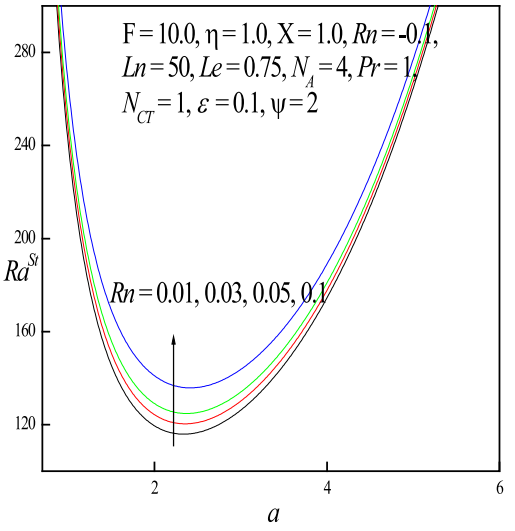

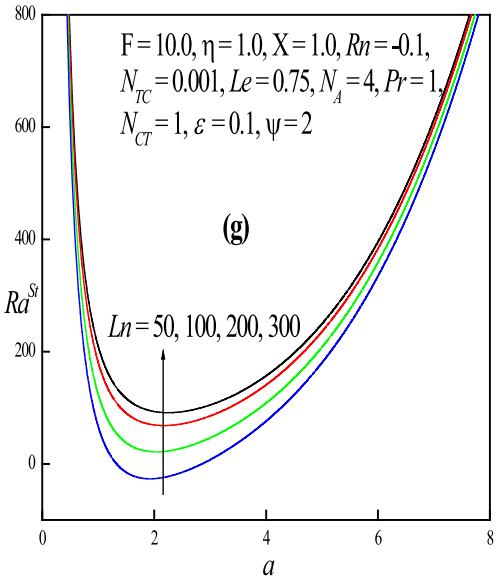

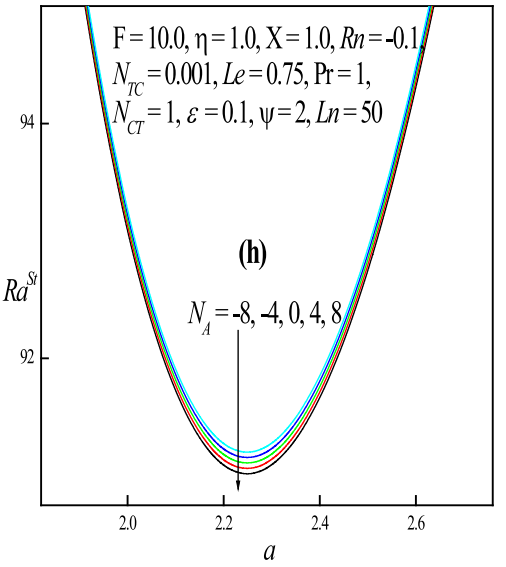

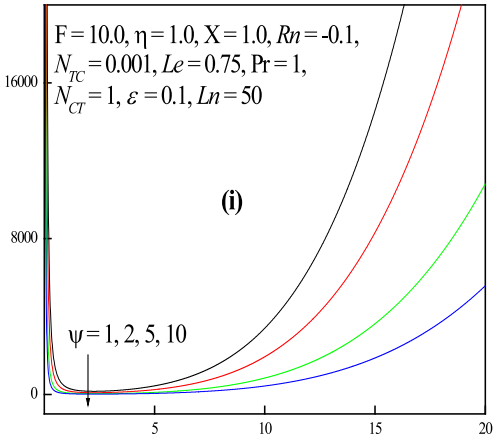

Fig. 2. (*continued*).

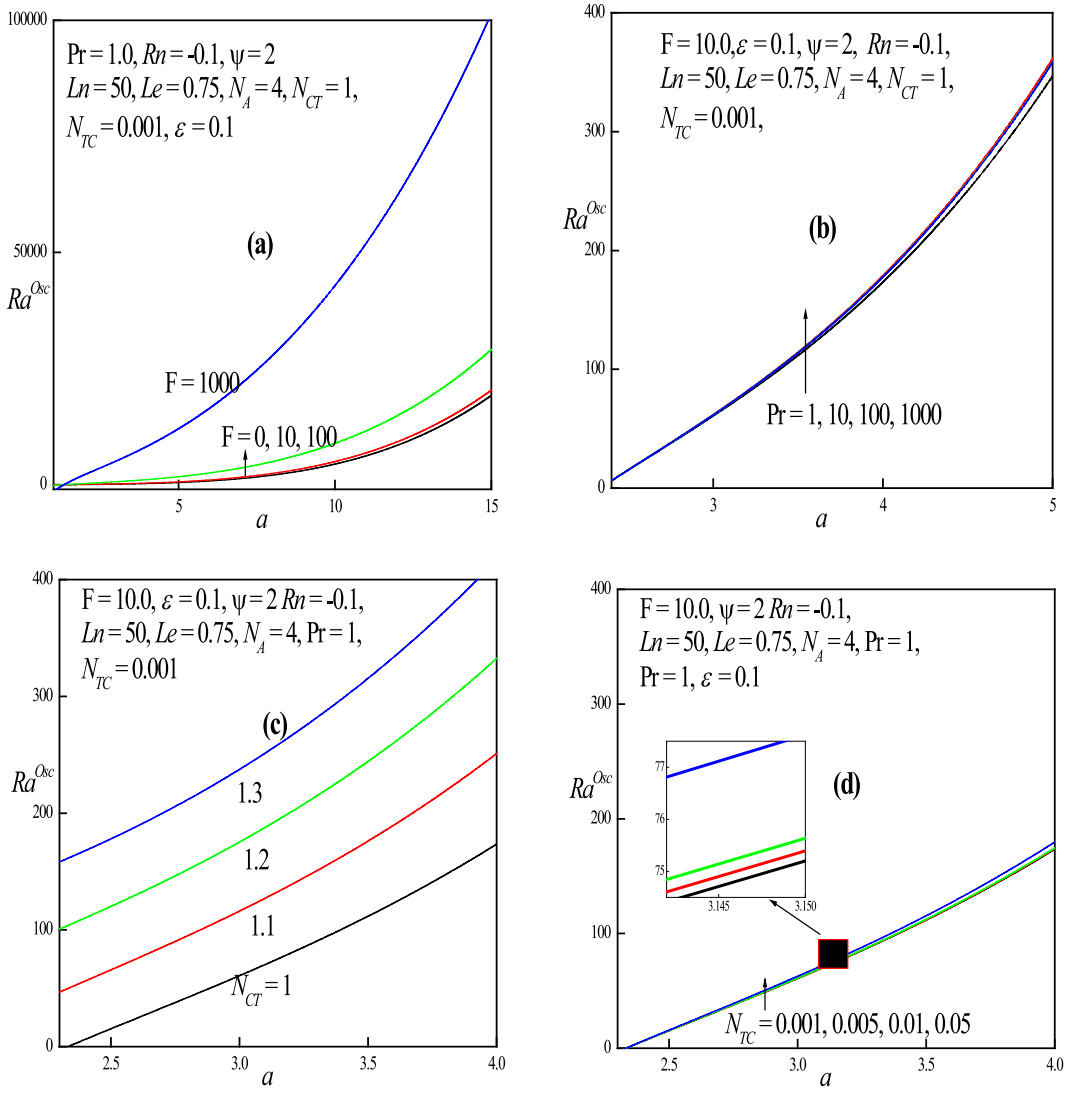

Fig. 3. Ra versus a for various **(a)** F **(b)** Pr **(c)** N_{CT} **(d)** N_{TC} **(e)** Rn **(f)** Ln **(g)** N_A and **(h)** ψ for the oscillatory case.

Malashetty and Gaikwad [32]. Figs. 3c and 3d represent the influence of Soret parameter N_{CT} and Dufour parameter N_{TC} on the Rayleigh number and it tells that as both N_{CT} and N_{TC} increase the Rayleigh number also increases for oscillatory convection. This physically implies that the onset of convection can be delayed by choosing appropriate values of N_{CT} and N_{TC}. As the solutal Rayleigh number R_n increases, the Rayleigh number is decreasing for oscillatory convection indicating that R_n will not help to stabilize the system as can be viewed in Fig. 3e. The Lewis number L_n follows the same property as that of solutal Rayleigh number. That is to say that L_n does not support the system to become stable as seen in Fig. 3f. The impact of diffusivity ratio N_A and chemical reaction parameter ψ also reduces the Rayleigh number as seen in Figs. 3g and 3h respectively. Hence N_A and ψ destabilize the system. The influence of all the above parameters for oscillatory convection was the similar results obtained by Malashetty and Gaikwad [32] for regular fluid and with Umavathi and Mohite [52] for nanofluid in the absence of chemical reaction parameter.

For the stationary and the oscillatory convection, the effects of the porous parameter F and η show the similar effect as noted by Malashetty and Gaikwad [32]. The influence of the N_{CT}, and N_{TC} is the identical result as observed by Umavathi and Mohite [52]. The parameters Rn, Ln, N_A show the identical profiles as observed by

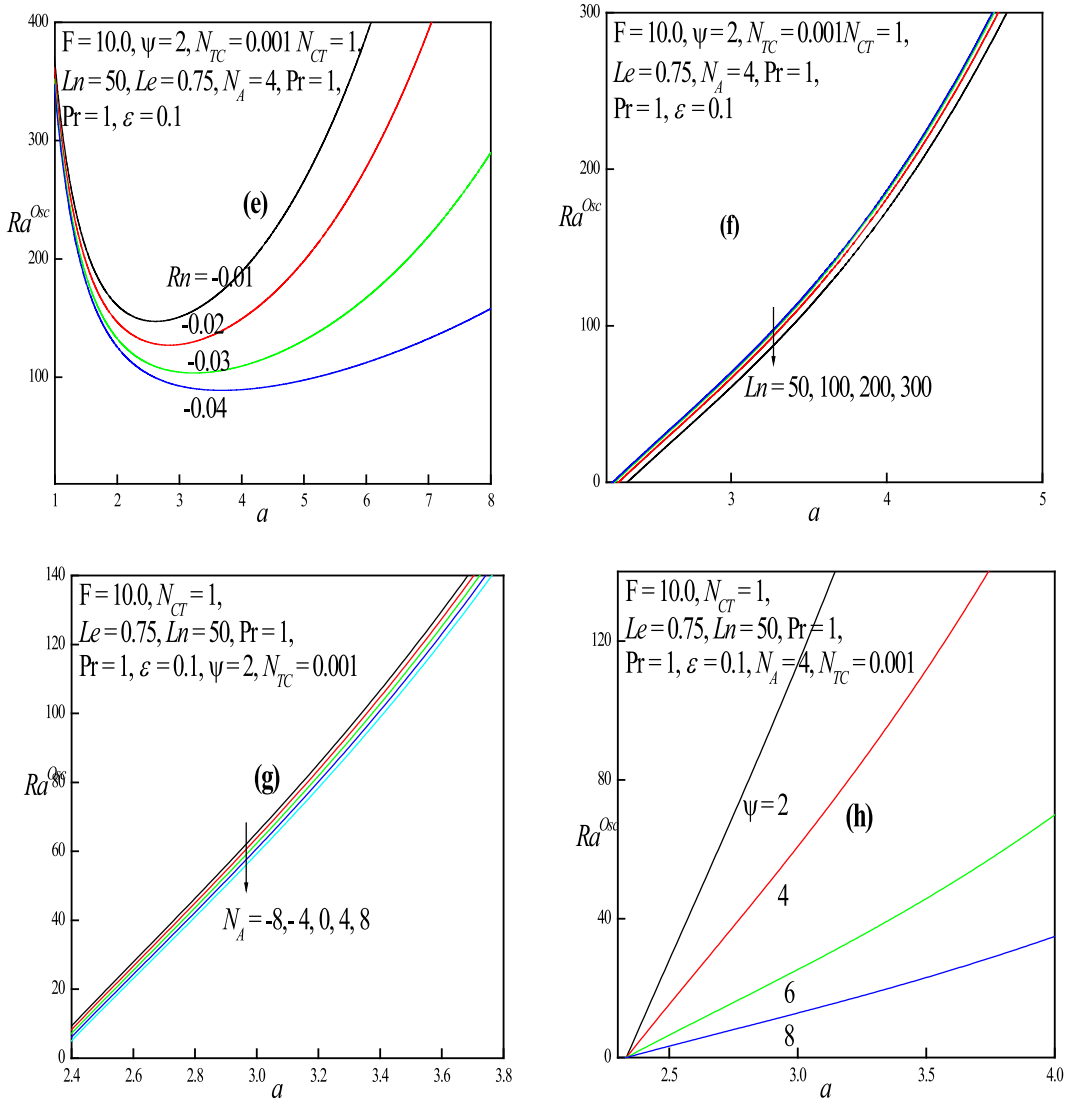

Fig. 3. (*continued*).

Umavathi and Mohite [53]. One can also identify from the stationary and oscillatory convection profiles that the chemical reaction parameter ψ assists to set back the onset of convection. By employing a nanofluid, we observe an enhancement in the Rayleigh number hinders the convection to set on. Our results are in agreement with those reported by Malashetty and Gaikwad [32] for $Rn = 0$, $Ln = 0$, $N_A = 0$ for regular fluid.

5. Conclusions

A binary mixture of a nanofluid saturated in a porous matrix with a fast chemical reaction filled inside a horizontal duct was considered to understand the stability of the system. The effects of thermophoresis and Brownian motion are also included. The stationary and oscillatory solutions are computed analytically. The rate of diffusion is assumed to be slow with respect to the rate of reaction. From the obtained results, we draw the following conclusions:

1. For the stationary mode, the porous parameter F, Soret parameter N_{CT}, Dufour parameter N_{TC}, and the Lewis number Ln have a stabilizing effect while η, solutal Rayleigh number Rn, modified diffusivity ratio N_A, and the chemical parameter ψ destabilize the system. The Prandtl number Pr has no influence for the stationary convection.

2. For the oscillatory mode, F, Pr, N_{CT}, and N_{TC} have the tendency to stabilize the system while Rn, Ln, N_A, and ψ do not stabilize the system.
3. For the stationary and the oscillatory convection, the effects of the porous parameter F and η show the similar effect as observed by Malashetty and Gaikwad [32] for regular fluid. The enforcement of N_{CT}, and N_{TC} on the onset of convection is the same result as observed by Umavathi and Mohite [52]. The parameters Rn, Ln and N_A show similar profiles as observed by Umavathi and Mohite [53].
4. By using a nanofluid, we observe an escalation in the Rayleigh number for both the stationary and the oscillatory convection and hence the nanofluid helps to advance the onset of convection.

The results of this work are relevant to the safe operation of an exothermic reactor during its shut-down period especially when a regular fluid is replaced with a nanofluid. Tubular reactors, oxidation of solid materials and synthesis of ceramic materials are also the practical applications which requires the understanding of stability analysis with chemical reactions in the presence of nanoparticles. Much work is still awaited on this topic using different types of nanofluids.

References

[1] S.Z. Abbas, M.I. Khan, S. Kadry, W.A. Khan, M. Israr-Ur-Rehman, M. Waqas, Fully developed entropy optimized second order velocity slip MHD nanofluid flow with activation energy, Comput. Methods Programs Biomed. (2020) http://dx.doi.org/10.1016/j.cmpb.2020.105362.

[2] S.Z. Abbas, W.A. Khan, S. Kadry, M.I. Khan, M. Waqas, M.I. Khan, Entropy optimized Darcy–Forchheimer nanofluid (Silicon dioxide, Molybdenum disulfide) subject to temperature dependent viscosity, Comput. Methods Programs Biomed. 190 (2020) 105363.

[3] A. Aziz, T. Muhammad, T. Hayat, A. Alsaedi, Influence of homogeneous-heterogeneous reactions in three-dimensional rotating flow of nanofluid subject to Darcy–Forchheimer porous medium: An optimal analysis, Phys. Scr. 94 (2019) 1157089.

[4] J.L. Beck, Convection in a box of porous material saturated with fluid, Phys. Fluids 15 (8) (1972) 1377–1383.

[5] B. Bhadauria, S. Agarwal, A. Kumar, Nonlinear two-dimensional convection in a nanofluid saturated porous medium, Transp. Porous Media 90 (2) (2011) 605–625.

[6] V. Bianco, O. Manca, S. Nardini, K. Vafai, Heat Transfer Enhancement with Nanofluids, Publisher CRC, Taylor and Francis Group, Boca Raton, FL, 2015.

[7] H.C. Brinkman, The viscosity of concentrated suspensions and solutions, J. Chem. Phys. 20 (1952) 571–581.

[8] J. Buongiorno, Convective transports in nanofluids, ASME J. Heat Transfer 128 (3) (2006) 240–250.

[9] R. Chand, G.C. Rana, Oscillating convection of nanofluid in porous medium, Transp. Porous Media 95 (2) (2012) 269–284.

[10] S.H. Davis, Convection in a box: Linear theory, J. Fluid Mech. 30 (3) (1967) 465–478.

[11] G. Diglio, C. Roselli, M. Sasso, J.C. Umavathi, Borehole heat exchanger with nanofluids as heat carrier, Geothermics 72 (2018) 112–123.

[12] J.A. Eastman, S.U.S. Choi, W. Li, S. Yu, L.J. Thompson, Anomalously increased effective thermal conductivities of ethylene-glycol-based nanofluids containing copper nanoparticles, Appl. Phys. Lett. 78 (6) (2001) 718–720.

[13] D.A. Frank-Kamenetskii, Diffusion and Heat Transfer in Chemical Kinetics, second ed., Plenum Press, New York, 1969.

[14] G.Z. Gershuni, E.M. Zhukovitskii, Convective Stability of Incompressible Fluids, Israel Program for Scientific Translations, Jerusalem, 1976.

[15] T. Hayat, A. Aziz, Numerical treatment for Darcy Forchheimer flow of nanofluid due to a rotating disk with convective heat and mass conditions, Int. J. Numer. Methods Heat Fluid Flow 28 (2018) 2531–2550.

[16] T. Hayat, A. Aziz, T. Muhamma, A. Alsaedi, Significance of homogeneous–heterogeneous reactions in Darcy–Forchheimer three-dimensional rotating flow of carbon nanotubes, J. Therm. Anal. Calorim. 139 (2020) 183–195.

[17] T. Hayat, A. Aziz, T. Muhammad, A. Alsaedi, Numerical simulation for Darcy–Forchheimer 3D rotating flow subject to binary chemical reaction and Arrhenius activation energy, J. Cent. South Univ. 26 (2019) 1250–1259.

[18] T. Hayat, A. Aziz, T. Muhammada, A. Alsaedi, On magnetohydrodynamic three-dimensional flow of nanofluid over a convectively heated nonlinear stretching surface, Int. J. Heat Mass Transfer 100 (2016) 566–572.

[19] T. Hayat, A. Aziz, T. Muhammada, A. Alsaedi, Numerical simulation for three dimensional flow of Carreau nanofluid over a nonlinear stretching surface with convective heat and mass conditions, J. Braz. Soc. Mech. Sci. Eng. 41 (2019) 55.

[20] T. Hayat, M.I. Khan, M. Farooq, A. Alsaedi, M. Waqas, T. Yasmeen, Impact of Cattaneo–Christov heat flux model in flow of variable thermal conductivity fluid over a variable thicked surface, Int. J. Heat Mass Transfer 99 (2016) 702–710.

[21] T. Hayat, R. Riaz, A. Aziz, A. Alsaedi, Analysis of entropy generation for MHD flow of third grade nanofluid over a nonlinear stretching surface embedded in a porous medium, Phys. Scr. 94 (2019) 125703.

[22] T. Hayat, R. Riaz, A. Aziz, A. Alsaedi, Influence of Arrhenius activation energy in MHD flow of third grade nanofluid over a nonlinear stretching surface with convective heat and mass conditions, Physica A 549 (2020) 124006.

[23] M. Ibrahim, M.I. Khan, Mathematical modeling and analysis of SWCNT-water and MWCNT-water flow over a stretchable sheet, Comput. Methods Programs Biomed. (2019) http://dx.doi.org/10.1016/j.cmpb.2019.105222.

[24] M.I. Khan, F. Alzahrani, A. Hobiny, Heat transport and nonlinear mixed convective nanomaterial slip flow of Walter-B fluid containing gyrotactic microorganisms, Alexandria Eng. J. 59 (2020) 1761–1769.

[25] M.I. Khan, Faris Alzahraniy, Activation energy and binary chemical reaction effect in nonlinear thermal radiative stagnation point flow of Walter-B nanouid: Numerical computations, Int. J. Mod. Phys. B 2050132 (16 pages) http://dx.doi.org/10.1142/S0217979220501325.
[26] M.I. Khan, M. Waqas, T. Hayat, A. Alsaedi, Colloidal study of Casson fluid with homogeneous-heterogeneous reactions, J. Colloid Interface Sci. (2017) http://dx.doi.org/10.1016/j.jcis.2017.03.024.
[27] M.I. Khan1, S. Qayyum, S. Kadry, W.A. Khan, S.Z. Abbas, Irreversibility analysis and heat transport in squeezing nanoliquid flow of non-Newtonian (Second Grade) fluid between infinite plates with activation energy, Arab. J. Sci. Eng. 45 (2020) 4939–4947.
[28] M.I. Khana, F. Alzahranib, A. Hobiny, Simulation and modeling of second order velocity slip flow of micropolar ferrofluid with Darcy–Forchheimer porous medium, J. Mater. Res. Technology 9 (2020) 7335–7340.
[29] M.I. Khana, F. Alzahranib, A. Hobinyb, Z. Ali, Modeling of Cattaneo–Christov double diffusions (CCDD) in williamson nanomaterial slip flow subject to porous medium, J. Mater. Res. Technol. 9 (2020) 6172–6177.
[30] K. Khanafer, K. Vafai, Applications of nanofluids in porous medium: a critical review, J. Therm. Anal. Calorim. 135 (2019) 1479–1492.
[31] E.R. Lapwood, Convection of fluids in porous media, Proc. Cambridge Philos. Soc. 44 (4) (1948) 508–521.
[32] M.S. Malashetty, S.N. Gaikwad, Onset of convective instabilities in a binary liquid mixture with fast chemical reactions in a porous medium, Heat Mass Transf. 39 (5–6) (2003) 415–420.
[33] S. Marudappa, J.C. Umavathi, Influence of viscous dissipation on non-Darcy mixed convection flow of nanofluid, Heat Transfer - Asian Res. 46 (2) (2017) 176–199.
[34] J.C. Maxwell, A Treatise on Electricity and Electricity and Magnetism, second ed., Oxford University Press, 1904.
[35] R. Muhammad, M.I. Khan, Magnetohydrodynamics (MHD) radiated nanomaterial viscous material flow by a curved surface with second order slip and entropy generation, Comput. Methods Programs Biomed. (2019) http://dx.doi.org/10.1016/j.cmpb.2019.105294.
[36] R. Muhammad, M.I. Khan, M. Jameel, N.B. Khan, Fully developed Darcy–Forchheimer mixed convective flow over a curved surface with activation energy and entropy generation, Comput. Methods Programs Biomed. (2019) http://dx.doi.org/10.1016/j.cmpb.2019.105298.
[37] M.K. Nayak, A.K.A. Hakeem, B. Ganga, M.I. Khan, M. Waqas, O.D. Makinde, Entropy optimized MHD 3D nanomaterial of non-Newtonian fluid: A combined approach to good absorber of solar energy and intensification of heat transport, Comput. Methods Programs Biomed. (2019) http://dx.doi.org/10.1016/j.cmpb.2019.105131.
[38] M.K. Nayaka, S. Shawb, M.I. Khanc, V.S. Pandeyd, M. Nazeerc, Flow and thermal analysis on Darcy–Forchheimer flow of copper–water nanofluid due to a rotating disk: A static and dynamic approach, J. Mater. Technol. 9 (2020) 7387–7408.
[39] D. Nield, A. Kuznetsov, Thermal instability in a porous medium layer saturated by nanofluid, Int. J. Heat Mass Transfer 52 (25–26) (2009) 5796–5801.
[40] H.A. Pakravan, M. Yaghoubi, Combined thermophoresis, Brownian motion and Dufour effects on natural convection of nanofluids, Int. J. Therm. Sci. 50 (3) (2011) 394–402.
[41] R.F. Probstein, Physicochemical Hydrodynamics, second ed., Wiley Interscience, Hoboken, NJ, 2003.
[42] N. Putra, W. Roetzel, S.K. Das, Natural convection of nanofluids, Heat Mass Transf. 39 (8–9) (2003) 775–784.
[43] N. Rudraiah, M.S. Malashetty, The influence of coupled molecular diffusion on double diffusive convection in a porous medium, ASME J. Heat Transfer 108 (4) (1986) 872–876.
[44] N. Rudraiah, P.K. Srimani, R. Friedrich, Thermohaline convection in a fluid saturated porous layer with linear gradients, in: Proceeding of the Seventh International Heat Transfer Conference, Hemisphere Publ Corp, Washington, DC, 1982, pp. 449–454.
[45] V. Steinberg, H. Brand, Convective instabilities of binary mixtures with fast chemical reaction in a porous medium, J. Chem. Phys. 78 (5) (1983) 2655–2660.
[46] R.K. Tiwari, M.K. Das, Heat transfer augmentation in a two-sided lid-driven differentially heated square cavity utilizing nanofluids, Int. Heat Mass Transfer 50 (2007) 2002–2018.
[47] J.C. Umavathi, Effect of modulation on the onset of thermal convection in a viscoelastic fluid-saturated nanofluid porous layer, Int. J. Eng. Res. Appl. 3 (5) (2013) 923–942.
[48] J.C. Umavathi, Effect of time-periodic boundary temperature on the onset of nanofluid convection in a layer of a saturated porous medium, Int. J. Phys. Math. Sci. 7 (1) (2013) 1430–1435.
[49] J.C. Umavathi, Rayleigh-Benard convection subject to time dependent wall temperature in a porous medium layer saturated by a nanofluid, Meccanica 50 (4) (2015) 981–994.
[50] J.C. Umavathi, A.J. Chamkha, M.B. Mohite, Convective transport in a nanofluid-saturated porous layer with cross diffusion and variation of viscosity and conductivity, Spec. Top. Rev. Porous Media 6 (1) (2015) 1–17.
[51] J.C. Umavathi, I.C. Liu, M.A. Sheremet, Convective heat transfer in a vertical rectangular duct filled with a nanofluid, Heat Transfer - Asian Res. 45 (7) (2016) 661–679.
[52] J.C. Umavathi, M.B. Mohite, Double-diffusive convective transport in a nanofluid-saturated porous layer with cross diffusion and variation of viscosity and conductivity, Heat Transfer - Asian Res. 43 (7) (2014) 628–652.
[53] J.C. Umavathi, M.B. Mohite, The onset of convection in a nanofluid saturated porous layer using Darcy model with cross diffusion, Meccanica 49 (5) (2014) 1159–1175.
[54] J.C. Umavathi, M.B. Mohite, Convective transport in a porous medium layer saturated with a Maxwell nanofluid, J. King Saud Univ., Eng. Sci. 28 (1) (2016) 56–68.
[55] J.C. Umavathi, O. Ojjela, K. Vajravelu, Numerical analysis of natural convective flow and heat transfer of nanofluids in a vertical rectangular duct using Darcy–Forchheimer–Brinkman model, Int. J. Therm. Sci. 111 (2017) 511–524.
[56] J.C. Umavathi, J. Prathap Kumar, Onset of convection in a porous medium layer saturated with an Oldroyd nanofluid, ASME J. Heat Transfer 139 (1) (2017) 012401.
[57] J.C. Umavathi, M.A. Sheremet, Influence of temperature dependent conductivity of a nanofluid in a vertical rectangular duct, Int. J. Non-Linear Mech. 78 (2016) 17–28.

[58] J.C. Umavathi, M.A. Sheremet, Onset of double-diffusive convection of a sparsely packed micropolar fluid in a porous medium layer saturated with a nanofluid, Microfluid. Nanofluid. 21 (7) (2017) 121–128.
[59] A. Varma, R. Aris, Stirred pots and empty tubes, in: L. Lapidus, N.R. Amundson (Eds.), Chemical Reactor Theory. A Review, Prentice-Hall, New Jersey, 1977 (Chap. 2).
[60] H.J. Viljoen, J.E. Gatica, V. Hlavacek, Bifurcation analysis of chemically driven convection, Chem. Eng. Sci. 45 (2) (1990) 503–517.
[61] H.J. Viljoen, V. Hlavacek, Chemically driven convection in a porous medium, AIChE J. 33 (8) (1987) 1344–1350.
[62] J. Wang, M.I. Khan, W.A. Khan, S.Z. Abbas, M.I. Khan, Transportation of heat generation/absorption and radiative heat flux in homogeneous-heterogeneous catalytic reactions of non-Newtonian fluid (Oldroyd-B model), Comput. Methods Programs Biomed. (2019) http://dx.doi.org/10.1016/j.cmpb.2019.105310.
[63] J. Wang, R. Muhammad, M.I. Khan, W.A. Khan, S.Z. Abbas, Entropy optimized MHD nanomaterial flow subject to variable thicked surface, Comput. Methods Programs Biomed. (2019) http://dx.doi.org/10.1016/j.cmpb.2019.105311.
[64] Ya.B. Zeldovich, D.A. Frank-Kamenetskii, Thermal theory of flame propagation, J. Phys. Chem. 12 (1938) 100–105.